2
Experimental Techniques

2.1 INTRODUCTION

This chapter focuses on the techniques utilized in the characterization of MoS_2, WS_2, CuO, Fe_2O_3, and multicomponent quasicrystal materials. Subsequently, a detailed discussion is presented on various characterization techniques, including XRD, Raman spectroscopy, XPS, AFM, SEM, TEM, and BET. These techniques are employed to analyze the morphology, structural attributes, optical properties, and electrical characteristics of the synthesized materials. Additionally, the chapter elaborates on the experimental procedures designed to study gas-sensing. The experimental setup and its functionality are thoroughly described, providing insights into the practical implementation of the research.

2.2 MATERIALS SYNTHESIS

Several physical and chemical methods have already been widely explored in the literature to synthesize metal oxide and 2D TMDC. These methods include several top-down methodologies such as mechanical exfoliation *(Gao et al., 2018)*, chemical exfoliation *(Zhang et al., 2019)*, electrochemical *(P. Yu et al., 2015)*, LASER ablation *(Altuwirqi, 2022)* and liquid-phase exfoliation (Jalili et al., 2019) and bottom-up approaches such as epitaxial growth, chemical vapor deposition (CVD) *(Y. Yu et al., 2013)*, Hydrothermal *(B. Yu et al., 2016)* Electrode deposition (W. Liu et al., 2023) etc. Among these, bottom-up techniques such as epitaxial growth and CVD can provide large-area highly crystalline and pure films, but typically require high-temperature processing, and high vacuum and hence, are complex and costly. On the other hand, top-up approaches like mechanical exfoliation are relatively simple and low-cost but are time-consuming and non-scalable. Hence, neither of these techniques can be employed for large-scale manufacturing of low-cost sensors. A detailed discussion of all these techniques has been summarized below. In this work, we focus on the liquid phase exfoliation (LPE) technique which is attractive mostly due to the simplicity of the process, low cost of fabrication, and scalability *(Jalili et al., 2019)*, *(Huo et al., 2015)*. Although it is difficult to segregate several layers in this process, it provides a large yield at rather a low cost, with varying numbers of crystalline layers. Importantly, it has been widely studied in the literature using theoretical (DFT studies) *(Ferreira et al., 2018)*. The defects created during liquid exfoliation at the edges influence the electronic and optical properties of the material and make the material sensitive to these molecules. The synthesis techniques classification is depicted in Figure 2.1.

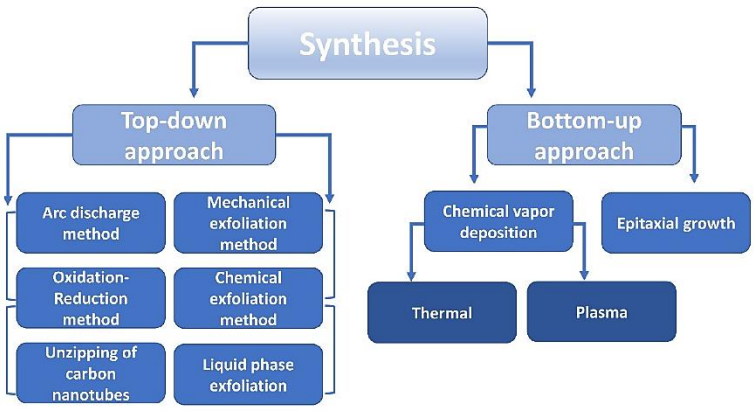

Figure 2.1: Different synthesis methods and techniques of materials development existing in the literature

2.2.1 Top-Down Approaches

2.2.1.1 Mechanical Exfoliation

The scotch-tape method first established by researchers in Manchester was the first known method for exfoliating a monolayer of carbon atoms from graphite. This micromechanical cleavage of graphite laid the foundation for the exfoliation of other layered materials like hexagonal Boron Nitride (h-BN), MXenes, TMDs, layered oxides, and hydrides, etc *(Balendhran et al., 2012)*, *(K. S. Kim et al., 2009)*. TMDs prepared using this method show good crystallinity with no defects. Hong et. al have prepared mechanically exfoliated p-WSe_2-based FET for the detection of different analytes such as NO_2, NH_3, SO_2, and H_2S (Y. Hong et al., 2017). MoS_2 and WSe_2 mono and a few layers were fabricated by using this technique and were deployed in phototransistors and gas sensors by Zhang's group*(H. Li, Wu, et al., 2014)*. Although this technique is relatively simple, the thickness-selective layers in very small islands (typically micron size) have to be identified through laborious statistical screening through visual inspection. Hence, it is a very time-consuming technique and provides low yield. Moreover, this is also not a scalable route for the manufacturing of low-cost gas sensors at an industrial scale. Therefore, this technique has been employed for only laboratory-grade nanostructures. Meanwhile, alternative approaches were developed to synthesize these nanomaterials at a large scale.

2.2.1.2 Liquid Exfoliation

Liquid phase exfoliation is a widely known top-down approach to disperse 2D materials from their bulk counterparts like Graphene, TMDs and 2D quasicrystal nanosheets, etc. effectively in liquid solvents. Ultrasonication used in this method aids in breaking the van der Waals bond with which these nanosheets are held together and results in mono to few-layered nanosheets. It is a well-known fact that if the surface energies of solvent and solute are similar, the energy difference will be negligible and hence the energy of exfoliation can be minimized. Hence, the minimization of energy using solvent-solvent, solute-solute, and solvent-solute binding energies can be optimized *(Coleman et al., 2009)*. Hansen's Solubility parameter (HSP) can be used to evaluate the level of adaptation between the HSP parameters of solvents and solutes. The HSP distance Ra, a semi-empirical parameter, is a measure of solubility. The lesser the Ra value, the more the solubility and vice-versa *(X. Liu et al., 2017)*. The HSP distance, Ra can be calculated using equation 1.1.

$$R_a = \sqrt{4(\delta_{D,\text{solvent}} - \delta_{D,\text{solute}})^2 + (\delta_{P,\text{solvent}} - \delta_{P,\text{solute}})^2 + (\delta_{H,\text{solvent}} - \delta_{H,\text{solute}})^2} \quad (2.1)$$

Where δD, δP and δH are dispersive, polar, and hydrogen bonding solubility parameters with the subscripts 'solvent' and 'solute' suggesting solubility parameters corresponding to solvent and WS_2 nanosheets respectively. Therefore, this theory aids in solvent selection and optimization. Exfoliation using organic solvents like N-methyl-pyrrolidinone (NMP), Benzyl alcohol, etc. is widely reported in literature by Coleman's group. Being high boiling point solvents (204°C), they sit on the surface of nanosheets and hamper the device's performance. Further, research efforts were invested in obtaining good yields in relatively lower boiling point solvents using a mixed solvent strategy *(K. G. Zhou et al., 2011)*. The value for δ for the mixture is given by equation 1.2

$$\delta_{mixture} = \sum_{i=1}^{n} \delta\phi_{solvent-i} - \delta_{solvent-i} \quad (2.2)$$

where $\delta_{mixture}$ is the total solubility parameter for the solvent mixture, φ_i is the volume fraction of ith solvent and δ_i is the individual solubility parameter.

Zhang's group demonstrated the exfoliation of MoS_2 in an optimized ratio of ethanol water *(K. G. Zhou et al., 2011)*. Nguyen and co-workers employed a grinding-assisted two-solvent sonication technique wherein grinding took place in a low boiling point solvent followed by subsequent exfoliation in ethanol *(H. Wang et al., 2022)*. Strano group have demonstrated surfactant-assisted exfoliation of graphene in solvent by using graphite intercalation compounds *(Shih et al., 2011)*. Eda et al. utilized ion intercalation to exfoliate MoS_2 layers for their application in photoluminescence *(Eda et al., 2011)*. Rao et. al reported Li ion intercalation-assisted exfoliation in hexane using n-butyllithium *(Ramakrishna Matte et al., 2010)* Further, electrochemical Li insertion was adopted by Zeng's group to exfoliate 2D materials like MoS_2, WS_2, TaS_2, graphite, TiS_2, in water or ethanol *(Zeng et al., 2011)* However, lithium intercalation can cause changes in the structure of 2D material. Ajayan's group synthesized an $Al_{66}Co_{17}Cu_{17}$ alloy, along with its subsequent exfoliation into two-dimensional (2D) decagonal quasicrystals (QC), following a systematic process inspired by methodologies used in the exfoliation of layered materials like MoS_2 *(Yadav et al., 2020b)*.

2.2.1.3 Electrochemical Exfoliation

Electrochemical exfoliation usually performed under convenient and controllable conditions, is one of the promising techniques to exfoliate 2D materials in a scalable fashion. This methodology includes cathodic exfoliation, cationic intercalation, and anodic oxidation. The layered bulk materials formed by weak out-of-plane van der Waals interactions can be separated by cations or anions intercalation under highly positive/negative charge. Anodic exfoliation is always carried out in aqueous solution while cathodic exfoliation is carried out under highly negative charge in an organic solution consisting of alkali metal ions or quaternary ammonium cations. Several important parameters such as electrical conductivity, defect density, and thickness can be tailored by modifying the electrochemical parameters (current/ voltage) or the electrolyte. This technique has been successfully employed in the exfoliation of materials like graphite, black phosphorus, transition-metal dichalcogenides (TMDs), graphitic carbon nitride, transition metal oxides, metal-organic framework (MOF) nanosheets and MXenes *(M. Zhao et al., 2024)* . The fabrication of monolayers of most of the 2D materials using this methodology is still a challenge.

2.2.1.4 LASER Ablation

Since 1987, the Laser ablation technique has been used for producing high-quality nanocrystals, carbon nanostructures, etc *(Radhakrishnan et al., 2007)*, *(Mortazavi et al., 2012)*. In recent years, it has been employed for the synthesis of graphene nanosheets from its bulk counterpart in a liquid nitrogen environment *(Mortazavi et al., 2012)*. Recently, Trusovas et al. utilized short-pulse laser irradiation to synthesize graphene layers in pinewood *(Trusovas et al., 2019)*. Moreover, it has been demonstrated by other groups that the number of layers can be controlled by tuning the duration of pulse laser treatment *(S. C. Xu et al., 2014)*. However, most of the research efforts involve complicated experimental arrangements such as the requirement for high vacuum, high or very low temperatures, and metal catalyst for deposition (Mortazavi et al., 2012), *(S. C. Xu et al., 2014)*. Therefore, the efforts have been directed towards simple, low-cost synthesis of high-quality nanosheets. Kumbhakar's group has recently demonstrated the synthesis of graphene layers using facile and scalable laser ablation techniques in liquid medium and ambient environments. It involved the utilization of a waste material i.e. dry cell Bulk Graphite electrode which aids in the reduction of cost and provides potential for large-scale production *(Pramanik et al., 2020)* Wu et. al took a green synthesis route to prepare fullerene-like MoS_2 nanoparticles using PLA (Pulsed Laser Ablation) in water. This is highly enticing in various biomedical applications including drug delivery, and cancer therapy due to its biocompatibility and good solubility *(H. Wu et al., 2011)*.

2.2.2 Bottom-Up Approaches

2.2.2.1 Chemical Vapor Deposition

Chemical Vapor Deposition is one of the mostly adopted bottom-up approaches for growing high crystal nano and the microstructured thin film of Metal Oxide (eg. CuO, ZnO) and 2D TMDC (eg. MoS_2, WS_2, SnS_2). It can be done using two different ways i.e. either by sulphurization of respective metal/metal oxide or vapor phase reaction of metal oxide and sulphur. Several groups reported large-scale growth of TMDs by chemical vapor reaction, however, it results in the formation of randomly distributed flakes rather than a continuous film. Najmaei's group synthesized triangular flakes of MoS_2 atomic layers using the vapor-phase reaction of MoO_3 and S powders. Wang et al. reported hexagonal geometries of MoS_2 atomic layers depending upon the spatial location of the silicon substrate *(Y. J. Cho et al., 2023)*. To precisely control the growth of layers over a large area, Yu et al. developed a new two-step method. Firstly, a thin film of transition metal (e.g. Mo, W, Nb, etc.) was deposited on the substrate (usually Si/SiO_2) which was followed by a thermal reaction of chalcogen (S, Se, Te) vapor with the former at high temperatures (300–700°C) *(Y. Yu et al., 2013)*. Metal-Organic CVD is another alternative way as first claimed by Eichfeld et al. for the large area growth of mono and few-layer WSe_2 using Metal-Organic CVD precursors *(Eichfeld et al., 2015)*. Recently, the growth of WSe_2 by the metal-organic CVD method has yielded the formation of WSe_2 monolayers with a few hundred nanometers to the largest size of 8 um domain sizes *(W. Choi et al., 2017)*. Therefore, the CVD technique can potentially give very high-quality thickness selective layered material with low defect density, but typically requires very high-temperature processing and incurs huge costs. Hence this process is not very suitable for low-cost gas sensors. Moreover, an additional step is required to transfer the 2D layers from the metal substrate to the target substrates. This may introduce impurities/defects into these layers and may also increase the difficulty in controlling the manufacturing process.

2.2.2.2 Atomic Layer Deposition

ALD is another alternative route to grow nanomaterials layer by layer via a controlled gas phase reaction of precursor with the substrate. Recently, 3L WSe_2 has been synthesized at 800°C over a large area using this method by employing WCl_6 and diethyl selenide (DESe) as precursors. It was deployed for the room temperature detection of NO_2 *(Ko et al., 2018)*. Another group adopted an indirect route to synthesize WS_2 layers i.e by firstly growing tungsten oxide followed by annealing it in an H_2S atmosphere *(Song et al., 2013)* Furthermore, several efforts were invested in lowering the growth temperature. One of the groups demonstrated the growth of WS_2 layers in a lower temperature regime (300–450oC) by using H_2 plasma as a reducing agent and WF_6 and H_2S as precursors *(Delabie et al., 2015)*. Although ALD is highly scalable and provides precise control over the thickness of layers, the use of sensitive precursors and expensive instrumentation is still a major concern.

2.2.2.3 Wet Chemical Routes Several

Bottom-up approaches include solution-based exfoliation techniques to provide large yields at low cost. These chemical exfoliation techniques include hydrothermal, solvothermal, colloidal synthesis, electrodeposition, sol-gel, and template-based synthesis. The hydrothermal synthesis method is of great significance for large-scale production at lower temperatures (100- 240°C). This technique involves the dissolution of chemical precursors in water and then placed in a steel container that can withstand high temperatures and pressure. It is a very useful technique when precursors do not dissolve at low temperatures *(Zhang et al., 2019)* . Many 2D materials have been prepared by this method, like MoS_2, WS_2, TiO_2, Rh. Colloidal synthesis is another simple and well-established precipitation-based wet chemistry process. In this technique, the solution of different ions is mixed to form insoluble precipitates under controlled temperature and pressure

(Nasilowski et al., 2016). Electrodeposition is another long-established technique to deposit layers on a conducting substrate using aqueous/non-aqueous electrolytes. This process is relatively inexpensive, and fast while providing flexibility in choice of substrate and scalable growth *(Ambrosi et al., 2018)*. Several reports have demonstrated successful exfoliation of layered/non-layered materials using these wet chemical techniques. Advantages of this method over physical crystal growth techniques include low temperature, low cost, high yield, and ease in fine-tuning reaction parameters.

2.3 CHARACTERIZATION TECHNIQUES

In this thesis, a variety of characterization techniques have been used. These techniques are briefly discussed as follows:

2.3.1 X-ray diffraction (XRD)

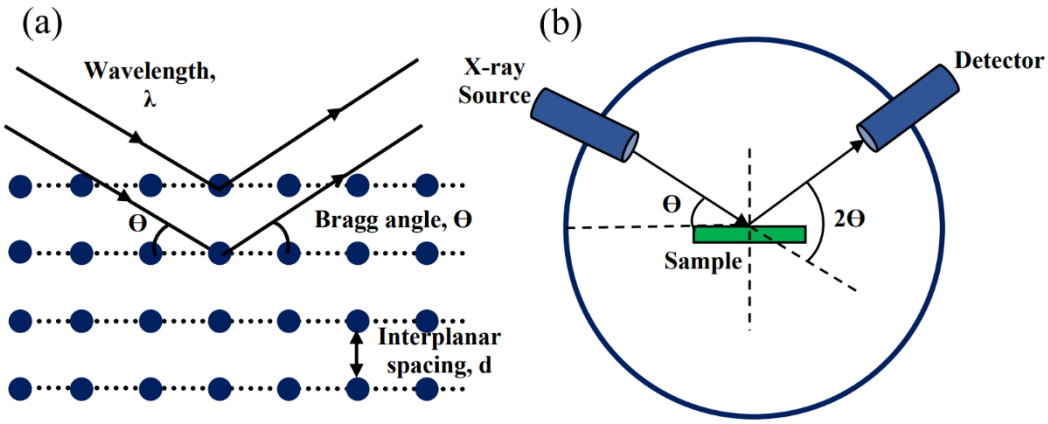

Figure 2.2: (a) X-ray reflection from crystal planes, **(b)** X-ray diffractometer setup. *(Mcewen et al., 2023)*

The crystallinity of the synthesized materials was characterized by the conventional powder X-ray diffraction (XRD) technique. XRD is a powerful analytical technique that is extensively used for the identification of crystalline material, and the determination of its unit cell parameters and phase. The basic principles of XRD and analysis of the same are well documented elsewhere. In brief, the basic principle is based on Bragg's Law. The Bragg equation relates the lattice spacing and diffraction angle between planes and is given by.

$$2d_{hkl}\sin(\theta) = n\lambda \qquad (2.2)$$

Where d_{hkl} is the lattice spacing of a plane (h k l), λ (Cu Kα, λ=1.5418 Å) is the wavelength of the incident X-ray photon, θ is the incident/glancing angle as shown in Figures 2.4 (a) and (b). n is the order of the diffraction pattern. The observation of the diffraction peaks is an indication of the crystalline nature of the material. The peaks correspond to the basic Bragg reflection belonging to a set of planes.

2.3.2 Electron microscopy studies

An electron microscope is a type of microscope that uses a beam of electrons to illuminate the specimen and produce a magnified image. Electron microscopes (EM) have a greater resolving power than a light-powered optical microscope because electrons have wavelengths about 100,000 times shorter than visible light (photons) and can achieve better than 50 pm resolution and magnifications of up to about 10,000,000x, whereas ordinary, non-confocal light microscopes are limited by diffraction to about 200 nm

resolution and useful magnifications below 2000x. When a high-energy electron beam is focused and allowed to interact with a solid medium, it undergoes several interesting phenomena. These phenomena are characteristic of the material of interest and can be utilized to characterize the material itself. Figure 2.3 shows the various possible phenomena that occur when an electron beam is focused on the material. The wave-particle duality exhibited by these electrons possesses a characteristic De Broglie wavelength depending on the acceleration voltage, which can be focused with the help of electromagnetic lenses and is effectively used in electron microscopes.

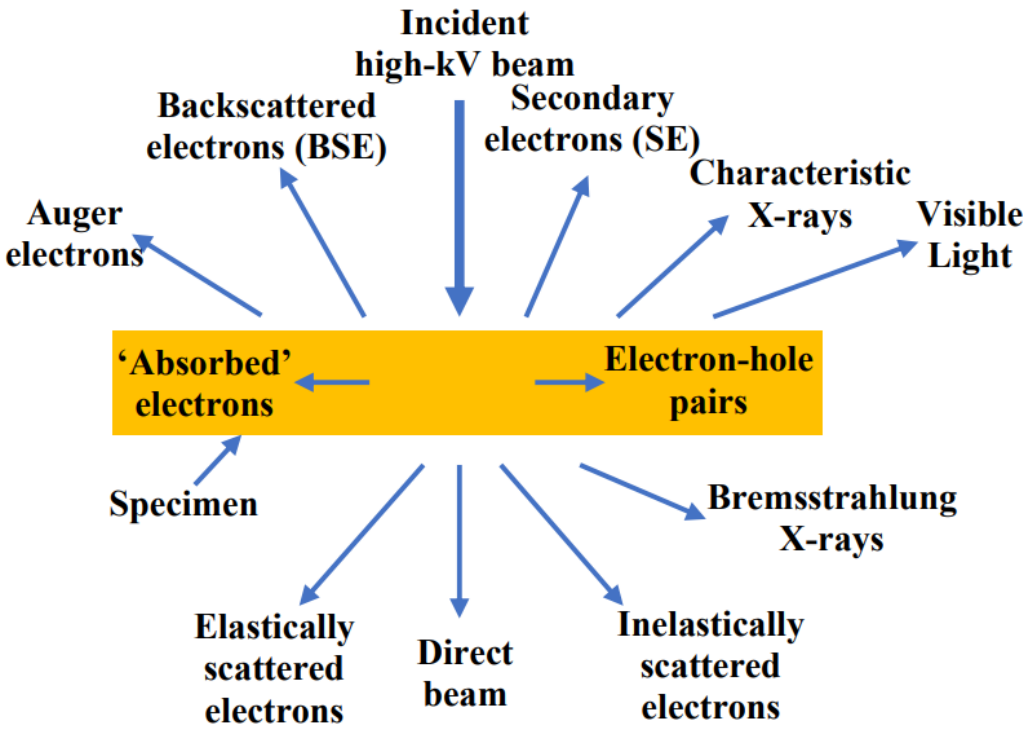

Figure 2.3: Electron specimen interactions.

2.2.3 Scanning electron microscopy (SEM) and energy-dispersive X-ray spectroscopy (EDS)

The scanning electron microscope (SEM) was designed for directly examining the surfaces of solid objects. In contrast to optical microscopy, which uses light to generate an image, electrons are responsible for image generation in SEM. A beam of high-energy electrons is fired onto the sample surface, causing many forms of interactions. Figure 2.4 depicts a simplified schematic of the SEM's inner structure compared to light microscopy. Signals from the sample surface are gathered to provide an informative picture. Based on the signal type, topological, chemical, and crystallographic information about the sample surface may be retrieved.

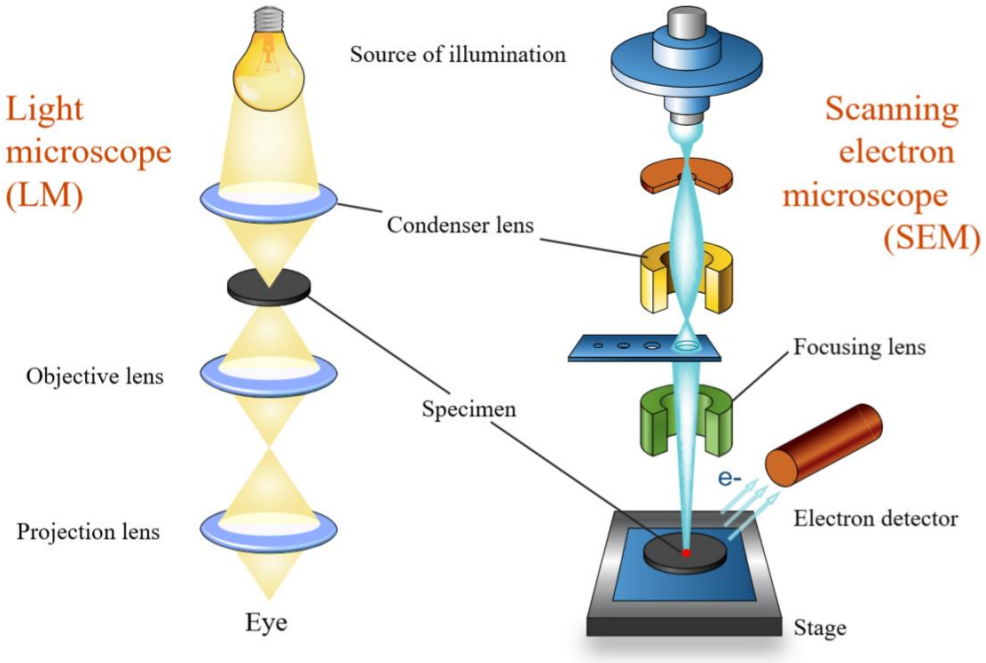

Figure 2.4: Basic structure and comparisons of Light microscope (LM) and Scanning electron microscope (SEM). *(Mcewen et al., 2023)*

Electrons penetrate the sample to a depth of about 1µm and interact elastically and inelastically with the solid, creating a limited interaction volume. Figure 2.5 depicts the many sorts of information carriers that may be formed within this bulb-shaped space. As schematically illustrated. They have various interaction volumes with the sample surface, which might affect SEM picture resolution.

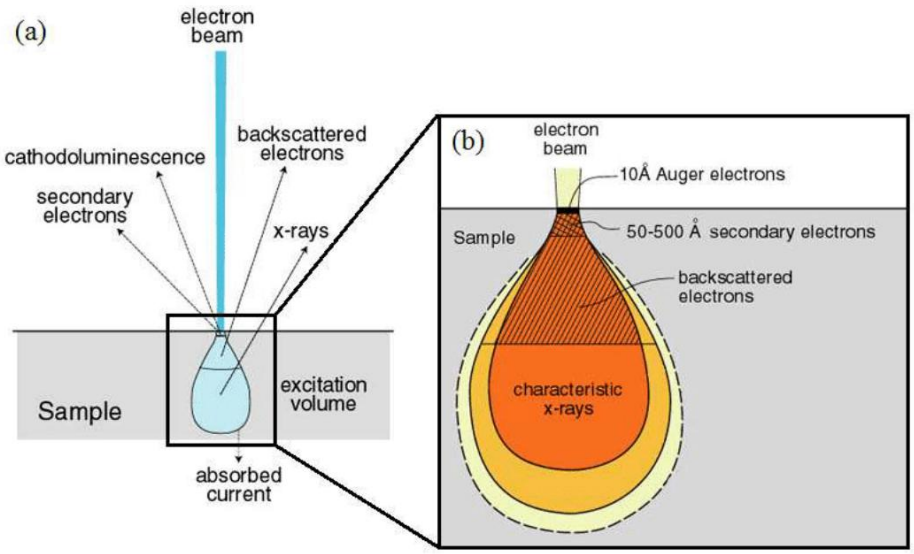

Figure 2.5: Diagram illustrating the phenomena resulting from the electron-sample interaction. *(Mcewen et al., 2023)*

SEM's principal signals are typically composed of backscattered electrons (BSE) and secondary electrons (SE). Backscattered electrons (BSE) typically have greater energies, approaching the energy of the incident electron beam. The intensity is essentially monotonic, increasing with atomic number, making it a very effective approach to convey compositional difference. Secondary electrons (SE) have lower energy (<5eV) and a smaller interaction volume (100Å). They might provide additional information on the topographic contrast of the sample surface. It is worth noting that both BSE and SE are dependent on the incidence angle between the beam and the sample. The same specimen might provide distinct pictures depending on the inclination

angle. As a result, fundamental knowledge and intuitive analysis are required for the assessment. Fluorescent X-rays are distinctive of many elements and are used to create energy-dispersive X-ray spectroscopy (EDS). The energy levels of each element change discretely. Each energy level might be utilized to fingerprint individual elements and create chemical composition data. In theory, atoms ranging in atomic number from 4 (Be) to 92 (U) can be discovered. Typical SEM measurements are performed under high vacuum conditions and need a conductive sample surface to avoid charging artifacts. Sample preparation is often simple for SEM measurement. If the sample surface is nonconductive, a layer of metal (e.g., gold-Au, platinum-Pt) or carbon film will be applied to improve image quality.

2.2.4 Transmission electron microscope (TEM)

Transmission electron microscope (TEM) is an extremely powerful tool in the characterization of materials crystal structure and microstructure simultaneously by diffraction and imaging up to atomic resolution. It is used to obtain information from samples that are thin enough to transmit electrons. The effects observed in the lower half of Figure 2.6 are utilized in characterizing the specimen. Transmitted electrons are generally used to form either an image or diffraction pattern (DP) of the specimen and a schematic of both the operational modes is shown in Figure 2.6. The transmitted electrons can also be used for microanalysis since the characteristic energy loss suffered by the electrons can be used to identify the elements present. A TEM in general has various condenser lenses, auxiliary and objective lenses, their functions, the convergence angles, their magnification, etc, are well known and documented elsewhere.

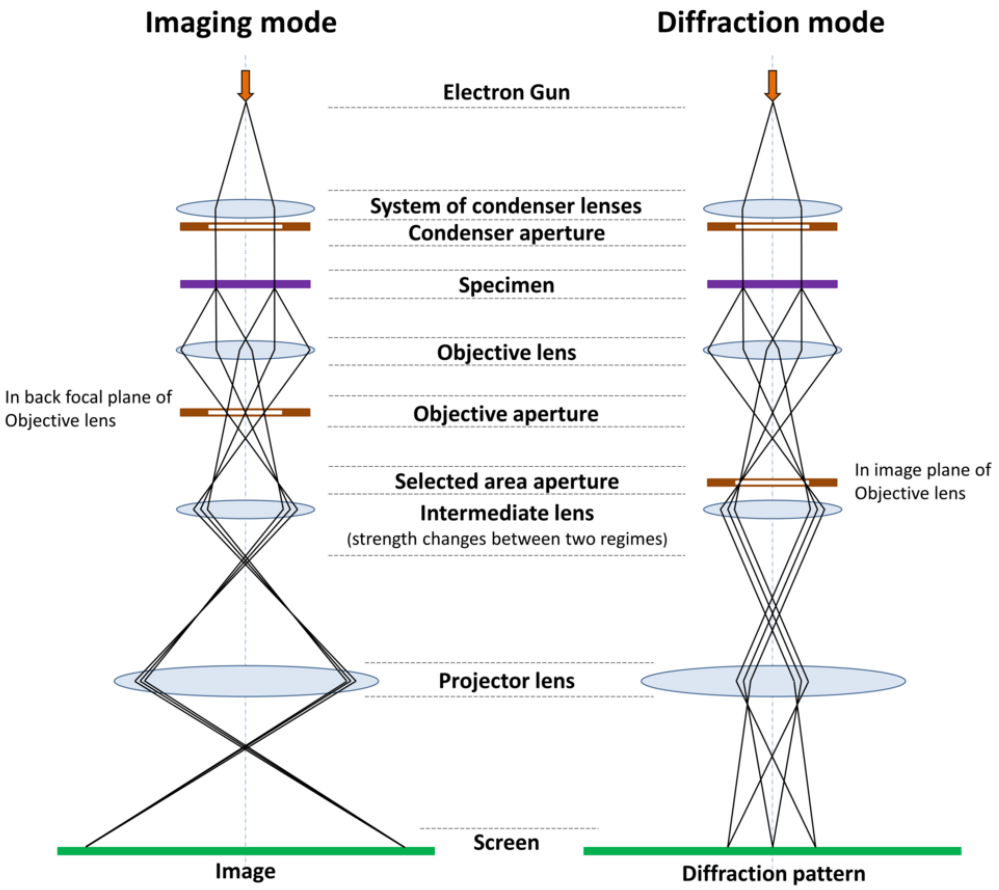

Figure 2.6: Schematic ray diagrams for diffraction pattern (a) and imaging (b) in TEM. *(Mcewen et al., 2023)*

In this thesis, a FEI Titan FEG high-resolution transmission electron microscope (HRTEM) operating at 300 kV was used to explore the microstructural details of the samples.

The absorption spectra of the samples were recorded using a dual-beam spectrophotometer (Thermo Scientific, Evolution 201).

2.3.5 Scanning Force Microscopy

Atomic force microscopy (AFM) is the most popular type of scanning probe microscopy (SPM). It was developed to get a probe close to the sample surface. The simplified schematic is presented in Figure 2.7. The force correlates with the cantilever's deflection. As the probe is scanned across the sample surface, their contact, indicated by force values, will be monitored as a function of position, allowing a picture of the sample surface configuration to be formed.

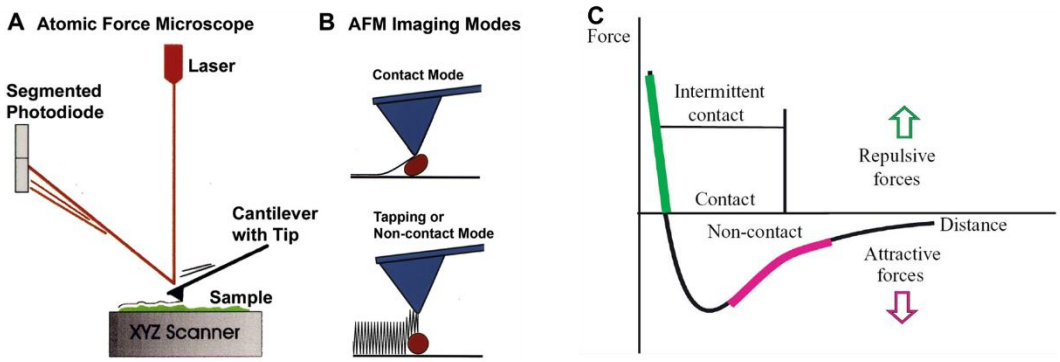

Figure 2.7: The schematic demonstrating the working principle of AFM. (b) AFM imaging modes: contact mode, non-contact mode, and tapping mode. (c) Curve demonstrating a force-distance relationship between the sample surface and the tip. *(Mcewen et al., 2023)*

AFM measurement has three imaging modes, which vary depending on the contact type and force acquisition design (Figure 2.7b). In the contact mode, the tip is continually in touch with the sample, and the force between the two is repulsive. A morphological image might be formed using the laser beam's deflection. In the non-contact mode, the tip and sample surface are kept at a constant distance, and image creation is done using amplitude based on phase deflection. The tapping mode combines the previous two modes, and the cantilever oscillates on the sample surface. Friction and adhesion forces may have a significant impact on contact mode, potentially causing surface damage. However, pollutants can also interfere with the non-contact mode, resulting in lesser-quality photos. Tapping mode makes use of the previous two modes. Intermittent contact with the sample surface would help to minimize friction and prevent getting trapped by the contaminated layer. Figure 2.7(c) illustrates the contact force between the sample surface and the AFM tip.

2.3.6 X-Ray photoelectron spectroscopy (XPS)

In photoelectron spectroscopy, the interaction known as the photoelectric effect is the process of prime importance. The photoelectric effect results in the emission of electrons from the extra nuclear cloud of core electrons, and valence electrons which are responsible for the binding of atoms together in molecules and solids. Photoelectrons emitted have kinetic energy, the magnitude of which is dependent upon both the photon energy (hv) and the energy possessed in the core. The measurement of this kinetic energy of the emitted photoelectrons is a necessary part of photoelectron spectroscopy. A simple absorption of radiation by matter can excite a system to its higher energy, a state generally named as excited state which is metastable. The excess energy possessed by the atom or a molecule due to its metastable state can relax through different processes to reach the ground state losing some energy. The various processes through which the system loses energy are luminescence, dissociation, degradation to vibrational energy, and electron emission. Thus, emitted electrons are different from those of photoelectrons and are alternatively known as autoionization or periodization. The electrons emitted due to the

relaxation of the system from a meta- stable state to attain the ground state is a two-step process and can even undergo more steps before electron emission. The photoelectric effect is a one-step process in which a photoelectron is emitted, and no intermediate steps are involved. The equation relating the kinetic energy of the photoelectron emitted and the probe beam can be written as

$$h\nu \rightarrow \text{Binding energy} + \text{Kinetic energy of photoelectron.}$$

The knowledge of the energy of the monochromatic probe beam used and the measurement of the kinetic energy of the photoelectron can give the binding energy of the emitted electron. This binding energy is the characteristic of the atomic species, chemical state, and the surrounding of the atomic species and can be a useful tool to characterize the atomic species in a molecule or a solid. The binding energy would be less in the case of valence electrons due to the screening effect produced by the core electron cloud and the binding energy of the core electron cloud is higher. The schematic of photoelectron generation is shown in Figure 2.8.

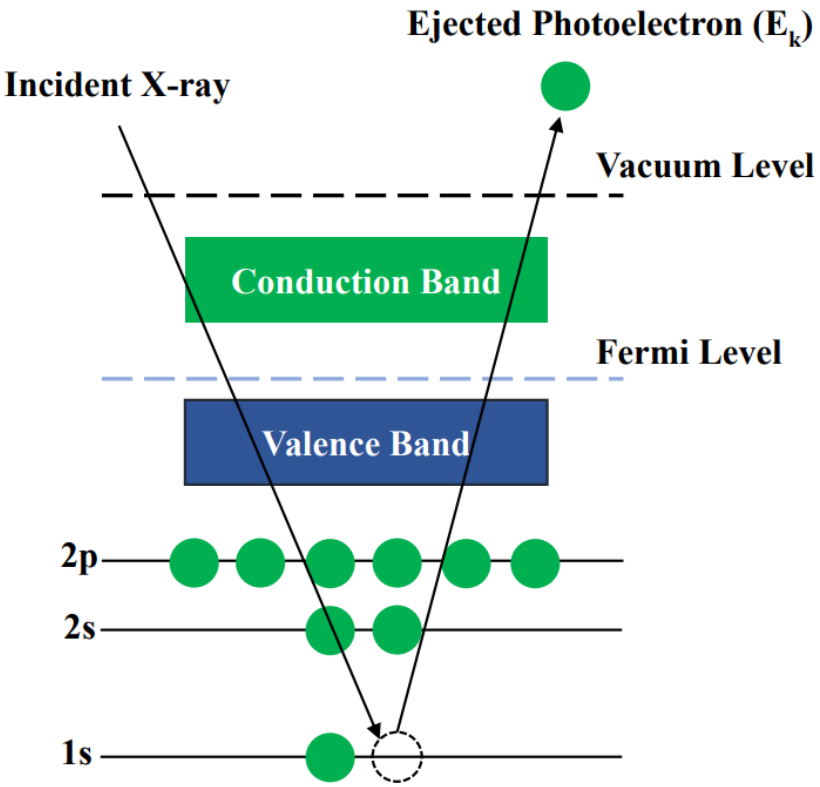

Figure 2.8: Schematic of photoelectron generation in XPS.

In this thesis, X-ray photoelectron spectroscopy analysis was done using a PHI 5000 VersaProb II, FEI Inc., equipped having an Al kα source (λ = 1.487 keV). The C1s peak at 284.60 eV was taken as a reference to correct the binding energy values of our samples.

2.3.7 Raman spectroscopy

Raman effect is an inelastic scattering of electromagnetic radiation by matter which was observed by Sir. C.V. Raman and the effect named after his name. The most considered example is that a monochromatic light of a certain frequency is inelastically scattered by a molecule and effectively produces scattered radiation both with higher and lower frequencies than that of the probe beam. The inelastic scattering is mainly due to the transition made by the molecule in its vibrational states. The higher frequency line observed is called anti-Stoke's line and the lower frequency line is Stoke's line. The whole process of Raman scattering is illustrated as shown in Figure 2.9.

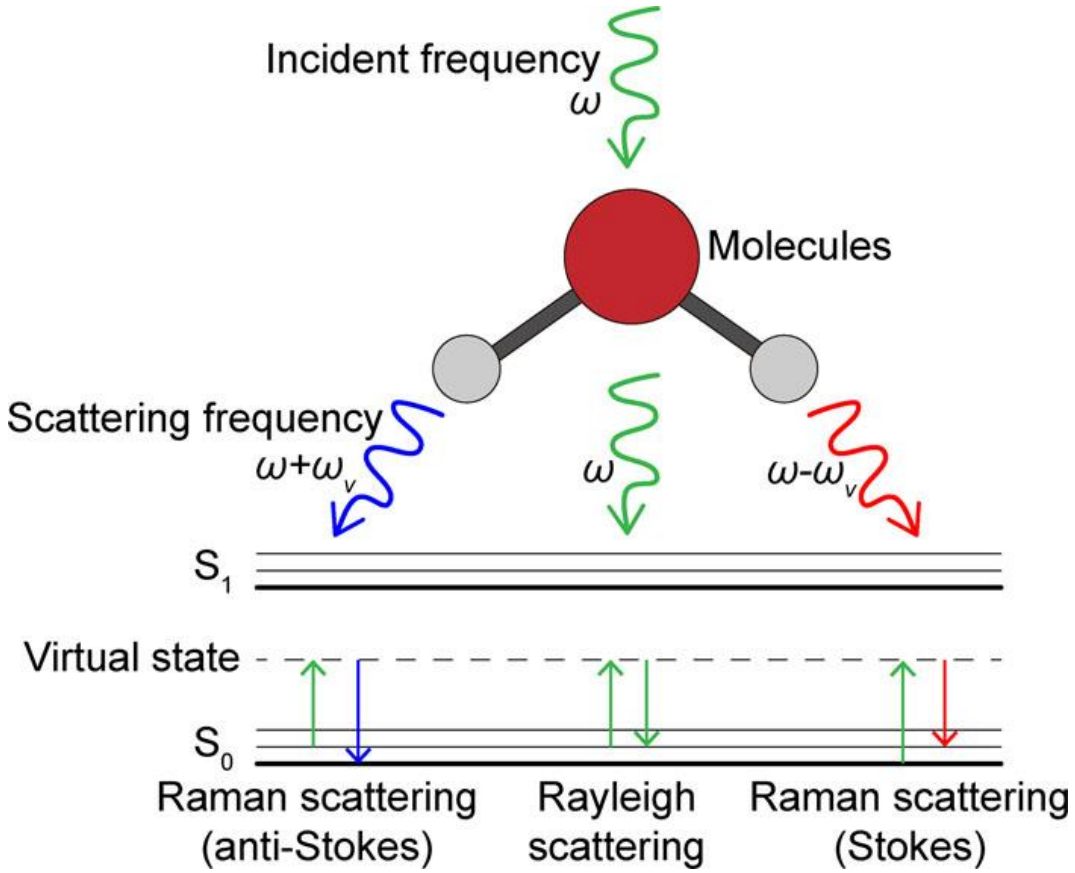

Figure 2.9: Schematic illustrating the Raman scattering phenomenon. *(Mcewen et al., 2023)*

The application of Raman scattering to characterize the phonon modes present in the crystalline solids is a well-established technique. In solid-state Raman scattering studies, the intense monochromatic light source mainly a laser, impinges over a solid and interacts with the collective excitations present in the medium. The interaction of the light with the collective excitations in the solid gives rise to a spectral distribution of frequencies. Appearance of a stokes line involves the emission of energy to the medium to create a phonon and anti-stokes lines involve absorption of energy from the medium in which annihilation of phonons in the medium takes place. The whole process of Raman scattering is identical to the inelastic scattering of X- rays. The selection rules for the first-order Raman effect are given as follows:

$$\omega=\omega' \pm \Omega \qquad (2.3)$$

$$k= k' \pm K \qquad (2.4)$$

Where ω, k refers to the incident photon frequency and wave vector respectively, ω', k' refers to the scattered photon frequency and wave-vector, and Ω, K refers to the phonon created or destroyed in the scattering event. In the second-order Raman effect, two phonons are involved in the inelastic scattering of the phonon.

In this thesis, samples were characterized by an inVia Renishaw Raman spectrometer was used for the Raman analysis, and incident laser light (532 nm) was used to determine the different vibrational modes.

2.3.8 Ultraviolet-visible spectroscopy (UV-vis study)

The principle behind UV-Visible (UV-Vis) spectroscopy is based on the interaction of molecules with light in the ultraviolet and visible regions of the electromagnetic spectrum. This technique relies on the fact that molecules absorb specific wavelengths of light due to electronic transitions.

When molecules absorb light in the UV or visible range, they transition from a ground state to an excited state. The absorption of light by molecules leads to changes in their electronic structure, which can be detected and analyzed through UV-Vis spectroscopy. In essence, UV-Vis spectroscopy measures the amount of discrete wavelengths of UV or visible light that are absorbed by a sample in comparison to a reference or blank sample. This absorption is influenced by the composition of the sample and provides valuable information about the components present and their concentrations. The technique is based on the energy required to promote electrons in a substance to a higher energy state, which results in the absorption of specific wavelengths of light corresponding to these electronic transitions. The Beer-Lambert Law is fundamental to UV-Vis spectroscopy, relating the concentration of a solution, the path length that light travels through the solution, and the absorbance of light by the solution. This law allows for the quantification of the sample's concentration by measuring its absorbance at specific wavelengths, providing a direct relationship between absorbance and concentration.

2.3.9 Fourier Transform Infrared Spectroscopy (FTIR)

In Fourier Transform Infrared (FTIR) Spectroscopy, vibrational spectroscopy is employed to analyze the local bonds within a composite material. When exposed to infrared (IR) radiation, molecules with a permanent dipole moment exhibit vibrations at characteristic frequencies corresponding to their vibrational modes. Even molecules without a permanent dipole moment can vibrate at specific frequencies. The reflected beams, resulting from the optical path difference between a fixed and a movable mirror, are directed through the sample. The light beam, now exhibiting frequency-dependent phase variations, is detected and converted into intensity variations using Fourier transform techniques, producing an interferogram. This interferogram is then processed using the Cooley-Tukey algorithm to generate a wavenumber-dependent spectrum. Compared to conventional IR spectrometers, FTIR offers higher resolution, faster data acquisition, and an improved signal-to-noise ratio.

2.3.10 BET (Brunauer-Emmett-Teller) method

The BET (Brunauer-Emmett-Teller) method serves as a crucial tool for determining the average surface area, pore volume, and pore diameter of solid materials through the physical adsorption of gas molecules on their surface. This technique relies on multilayer adsorption and employs gases that do not chemically react with the sample surfaces as adsorbates. Typically, nitrogen (N_2) is utilized as the probing gas at its boiling temperature (77 K) during BET spectroscopy. Although the concept of adsorption is rooted in Langmuir's theory of monolayer adsorption, in practice, the experiment follows multilayer adsorption processes.

Table 2.1 Comparative Summary of Characterization Techniques:

Technique	Resolution	Purpose	Advantages	Limitations
Scanning Electron Microscopy (SEM)	~1–10 nm	Surface morphology, particle size, film uniformity	High spatial resolution; fast imaging; easy sample prep	Limited to surface; requires conductive coating for non-conductive samples
Transmission Electron Microscopy (TEM)	<1 nm	Internal structure, crystallography, defects	Atomic-scale resolution; crystallographic and compositional info via SAED and EDS	Expensive; complex sample prep; requires ultrathin samples

X-ray Diffraction (XRD)	~0.1° in 2θ	Phase identification, crystal structure, crystallite size	Non-destructive; quantitative phase analysis; grain size via Scherrer formula	Limited to crystalline materials; less sensitive to amorphous content
Raman Spectroscopy	~1 µm	Vibrational modes, phase identification, disorder in carbon materials	Non-destructive; sensitive to carbon bonding (e.g., D/G bands in CNTs)	Fluorescence background; low sensitivity for metals
X-ray Photoelectron Spectroscopy (XPS)	~10 nm (surface)	Elemental composition, oxidation states, chemical bonding	Surface-sensitive; chemical state identification	Requires vacuum; shallow probing depth; time-consuming
Fourier-Transform Infrared Spectroscopy (FTIR)	~1–10 µm	Functional group identification (organic/inorganic)	Fast; simple; qualitative info on bonding	Overlapping peaks; less quantitative
Atomic Force Microscopy (AFM)	~1 nm (lateral), <1 nm (vertical)	Surface topology, roughness, nanomechanical properties	3D surface info; works in air/liquid; non-destructive	Small scan area; slow imaging speed
BET Surface Area Analysis	~0.01 m^2/g (detection limit)	Measurement of specific surface area, pore volume, and pore size	Provides quantitative data on porosity and surface area; essential for gas adsorption materials	Requires degassing; cannot provide morphology or elemental info
UV-Visible Spectroscopy	~1 nm (wavelength resolution)	Bandgap estimation, optical absorption	Simple; useful for bandgap and transitions	Limited to optically active materials; low depth info